Molecular-dynamics study of compressive stress generation

N. A. Marks, D. R. McKenzie, and B. A. Pailthorpe
School of Physics, University of Sydney, New South Wales 2006, Australia
(Received 11 August 1995)

The relationship between the ion-beam energy and the stress in thin carbon films is studied using two-dimensional molecular-dynamics simulations. In agreement with experiment, a transition is seen from tensile to compressive stress with increasing ion energy. The compressive stress reaches a maximum near 30 eV, after which it slowly decreases. A significant result of the simulations is that the compressive stress does not arise from the implantation of ions beneath the surface layer as has been previously proposed, rather, incident ions are incorporated into growing surface layers. Animation sequences of the impact process also provide detailed insight into the film growth mechanism.

I. INTRODUCTION

It is well established that the properties of thin films grown by deposition from ion beams are strongly dependent on the energy of the ions. Films grown with thermal energy ions are typically porous and have a columnar structure, whereas films grown with 30–100 eV ions have a dense, connected structure and are often compressively stressed. The compressive stress is of considerable interest as it causes delamination if the film is grown beyond a critical thickness and has also been linked to the formation of dense phases of materials such as tetrahedral amorphous carbon (ta-C) (Ref. 1) and cubic boron nitride.[2] This paper reports results of two-dimensional molecular-dynamics simulations designed to investigate the compressive stress generation mechanism.

In a number of materials the stress changes from tensile to compressive with increasing ion energy. A maximum compressive stress is attained for ion energies in the 40–70 eV range and above this energy the stress slowly decreases. Theories of compressive stress generation typically focus on two main areas, the mechanism by which the stress is generated and the dependence of the stress on the ion energy. Davis[3] has proposed a theory to explain the energy dependence of the stress and Robertson[4] has proposed a similar theory to explain the dependence of the sp^3 fraction in ta-C on the ion energy. Central to both theories is a conceptual picture of film growth known as the ''subplantation model.'' In this model the energetic ions are implanted into the subsurface of the film, producing densification and compressive stress in the process. In addition to this subplantation process, it is postulated that the ions cause local melting near the impact site, a phenomenon known as a ''thermal spike'' which anneals the surface region and reduces the stress. In the theories of Davis and Robertson it is the competing effects of densification and annealing which are responsible for the energy dependence of the compressive stress. While both theories are in reasonable agreement with experiment it has yet to be shown that subplantation mechanism is responsible for the generation of the compressive stress.

Molecular dynamics (MD) is a highly effective technique for understanding film growth because the film and substrate are treated from an atomistic perspective. Implantation models such as TRIM are valid only when the ion energy is over 100 eV as they assume the binary collision approximation and picture the system from a continuum viewpoint. Müller[5] has successfully used MD to model the growth of films in two dimensions using thermal energy ions. Müller's simulations reproduced a number of experimentally observed features including columnar growth of the films, an increase in densification with energy, and a characteristic peak in the tensile stress for ions with an energy of 1–2 eV. However, these simulations were not suitable for the investigation of compressive stress phenomena.

At higher impact energies Kaukonen and Nieminen[6] had some success modeling the growth of carbon films. Using a Tersoff potential,[7] they found the films were most diamondlike when the ion energy was in the range 40–70 eV. However, their maximum sp^3 fraction was 44 %, approximately half of the experimentally observed value[1] and the stress in the films was not calculated. Simulations of individual ion beam impacts have also been performed for carbon[8] and silicon.[9] However, a common feature of all these simulations is a lack of detail concerning the thermal spike and the growth process itself. Both of these phenomena are studied in some depth in this work.

The simulations performed in this work reproduce experimentally observed features such as the transition from tensile to compressive stress with increasing energy and a peak in the compressive stress around 30 eV. A significant result of the simulations is that the compressive stress in the films is not due to subplantation. In fact, it was found that the energetic ions did not penetrate the surface at all. Instead they were incorporated into the surface layer of the film.

II. MODEL

A. The potential

The simulations were two dimensional and used a modified form of the Stillinger and Weber (SW) potential[10] to describe the atomic interactions. The parameters used were derived by Bensan,[11] who performed Hartree-Fock calculations to reparametrize the SW potential for graphite. The most important quantities were

$$\varepsilon = 5.5 \text{ eV}, \quad \sigma = 1.266 \text{ Å}, \quad \text{and} \quad \theta = 120°,$$

where ε is the bond strength, $2^{1/6}\sigma = 1.421$ Å is the bond length, and θ is the ideal bond angle.

The SW potential was chosen for this work as it offered the prospect of compressive stress in two dimensions. Previous 2D studies using the Lennard-Jones potential produced crystalline and polycrystalline films but not amorphous structures. In addition, the Lennard-Jones films were able to sustain a compressive stress only when an impurity atom was introduced into the system.[12] In this context the use of the SW potential is an attempt to simulate the growth of 2D films, which are both amorphous and intrinsically stressed.

It must be emphasized that the simulations are not an attempt to reproduce the dynamics of a particular material such as carbon, in either its graphite or diamond form. Instead, it should be viewed as a 2D model of a hypothetical material using a realistic interatomic potential. The restriction to two dimensions allowed a much larger system to be studied and a greater number of simulations to be performed. We are confident that the 2D nature of the calculation does not adversely affect the compressive stress phenomena as Müller[5] and others[12] have had success modeling tensile stress properties in two dimensions. In addition, the degree to which the results are consistent with experiment suggests the 2D model retains the essential characteristics of a thin film grown using an ion beam.

B. Growing the films

The simulation technique used to grow the films was chosen to emulate experimental conditions as much as possible. The ions were deposited individually, a thermostat was used to remove energy from the edge of the simulation cell, and the film and substrate were cooled back to 300 K before subsequent ions were deposited. It was not possible to model thermally activated processes such as surface diffusion as these occur on time scales of μs, which are too long to be simulated by MD.

The films were grown on a graphitelike substrate measuring 23×80 Å containing 736 carbon atoms. The ions were deposited randomly with normal incidence onto the central region of the substrate. The width of the ion beam was 40 Å. Periodic boundary conditions were not used, instead the edge atoms and the base layer were fixed.

To avoid prematurely chilling the thermal spike, the system was cooled to 300 K only once the structure was constant and no new bonds were being broken or formed. The typical lifetime of the spike before the cooling to 300 K ranged from 0.2 ps for the 1 eV ions to 1 ps for the 100 eV ions. The ions were deposited individually as even in rapid deposition systems such as the cathodic arc[13] the time between successive impacts in a 10×10 Å region is of the order of a millisecond. Thus the impact region reaches thermal equilibrium with the rest of the film and substrate long before the next ion arrives at the surface.

C. Calculating the stress and density

The lateral stress in the film was calculated using the following expression, which sums over all atoms in the film:

$$\sigma_{xx}=\frac{1}{A}\sum_{i<j}\frac{F(r_{ij})}{r_{ij}}(\triangle x_{ij})^2. \tag{1}$$

This definition is equivalent to calculating the force acting across vertical lines of arbitrary x position and taking the average value. In this expression, A is the area of the film, r_{ij} is the distance between atoms i and j, $F(r_{ij})$ is the force between atoms i and j, and $\triangle x_{ij}$ is the difference in x position of atoms i and j. The sign convention adopted for the force was positive for attraction and negative for repulsion. Thus a positive σ_{xx} indicates a tensile stress and a negative sign a compressive stress. Note that the units of σ_{xx} are not Pa but Nm^{-1} as a stress in two dimensions is a force per unit length. To assist in interpreting the magnitude of the stresses, σ_{xx} was converted to an equivalent three-dimensional value by dividing by 3.51 Å, the c-axis spacing in graphite. This equivalent value should be taken as a guide only.

It is instructive to rewrite Eq. (1) in the equivalent form

$$\sigma_{xx}\equiv\frac{\rho}{n}\frac{1}{2}\sum_i\sum_{j\neq i}\frac{F(r_{ij})}{r_{ij}}(\triangle x_{ij})^2=\frac{1}{n}\sum_i\sigma_i, \tag{2}$$

where

$$\sigma_i=\frac{\rho}{2}\sum_{j\neq i}\frac{F(r_{ij})}{r_{ij}}(\triangle x_{ij})^2, \tag{3}$$

n is the number of atoms in the region, and ρ is the atom number density/unit area. In this form σ_{xx} is expressed as the average value of a new quantity σ_i which measures the contribution of each atom i to the total stress. Thus σ_i represents the stress environment local to each atom.

The density was inferred from the average bond length r_{av} using the relation $\rho\sim1/r_{\mathrm{av}}^2$ and normalized with the graphite natural bond length, 1.421 Å. This expression provides a valid comparison between structures with similar topologies but different densities. This definition gave the most appropriate measurement of the density. Approaches based on counting the number of atoms in a given region were found to be overly sensitive to the area of the region specified.

III. RESULTS

A. General properties of the films

A total of six films, each containing between 300 and 400 atoms, were grown with ion energies of 1, 10, 20, 30, 50, and 75 eV. The films were amorphous and stressed and the film properties showed a strong dependence on the ion energy. In addition, the film grown with 75 eV ions was bombarded with two-hundred 100 eV ions, sufficient to result in another equilibrium stress level.

Four of the films are shown in Fig. 1, with the black and white circles denoting deposited ions and substrate atoms, respectively. The dependence of the stress and density on the ion energy is shown in Figs. 2 and 3. The error bars in Fig. 2 reflect the degree of uncertainty in the curve fit used to take into account fluctuations in the stress with film thickness. An example of the amorphous nature of the films is seen in Fig. 4, which shows the topology of the 75 eV film.

These figures show that the simulation reproduces the significant features observed experimentally. With increasing energy there is a transition from the voided columnar films under tensile stress to denser, more uniform films under com-

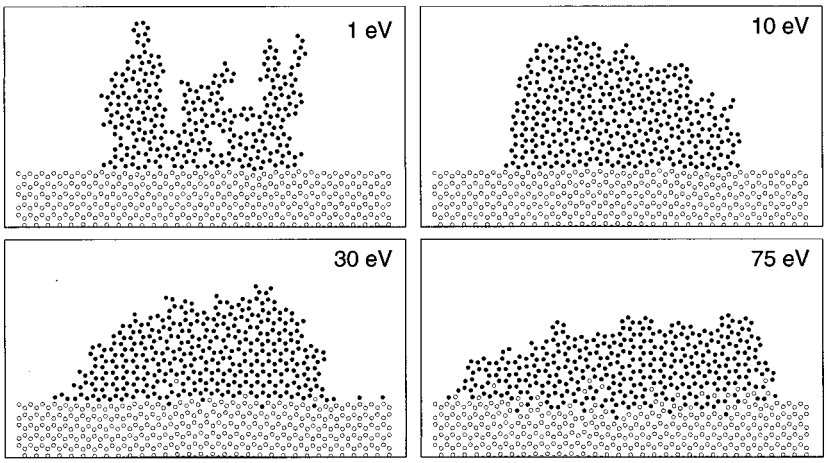

FIG. 1. Films grown with ion beam energies of 1, 10, 30, and 75 eV. The solid circles denote deposited ions while the white circles indicate substrate atoms.

pressive stress. At higher energies the stress reaches a maximum and then gradually decreases. This transition has not been previously reproduced in a simulation, but is commonly observed experimentally.

This dramatic change in morphology and properties is a function of the various dynamical processes which occur when the ions impact on the surface of the growing film. A 1 eV ion bonds to the first atom it comes near to, as its kinetic energy is insufficient to break bonds. For this reason the film growth is columnlike as higher sections of the film ''shadow'' the surrounding region. However, when 10 eV ions hit the surface, they have sufficient energy to break bonds, which prevents the growth of columns and produces a structure which is stress-free. As the ion energy is further increased, the films grow with significant compressive stresses. The mechanism by which this stress arises is quite subtle and is examined in detail in the following sections. At still higher energies, the stress decreases. Increased surface mobility is evident at these ion energies and the films in Fig. 1 show two consequences of this effect. As the ion energy increases the films become progressively wider and a greater degree of mixing occurs between the film (black circles) and the substrate (white circles).

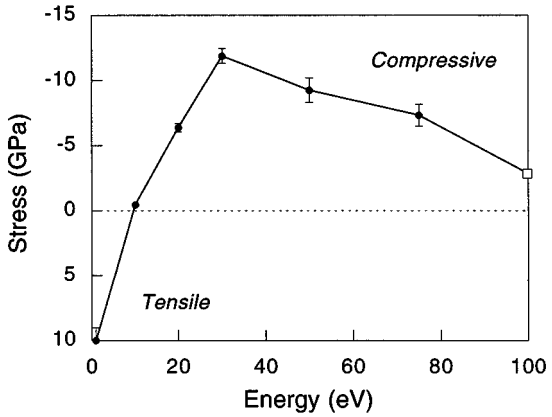

FIG. 2. Lateral stress in the simulated films as a function of the incident ion energy. The solid circles indicate films which were grown. The white square shows the stress of the film grown with 75 eV ions after it was bombarded with two hundred 100 eV ions.

B. Testing the subplantation model

Analysis of the thermal spike showed that the deposition process differs from the subplantation model proposed by Davis[3] and Robertson.[4] We propose a model in which energetic ions insert themselves into the growing surface while simultaneously heating the atoms near the impact site. Evidence for this model is presented below.

A critical test of whether subplantation is taking place is seen in Fig. 5, which shows the resting position of the energetic ions once the thermal spike has cooled. The final position of the ion ranges from outside of the film as a result of sputtering (white circle), to lying on the surface with various coordinations (solid markers), to becoming part of the bulk (white squares). The distinction between surface and bulk was made using the convention shown in Fig. 6, which used a ring counting algorithm to identify the surface and bulk regions. Atoms were deemed bulk atoms if they were found in three rings and surface atoms if in less than three rings. Bonds were considered to be in the bulk if they were found in two rings and as on the surface if in one ring or no ring at all. This definition of surface and bulk is used for the remainder of the paper.

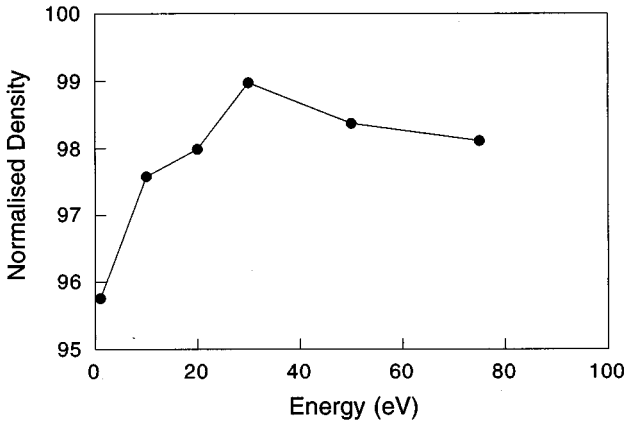

FIG. 3. Density of the simulated films as a function of the incident ion energy. The density was inferred from the average bond length and normalized using the graphite natural bond length. The values quoted are a percentage fraction of the natural density of graphite.

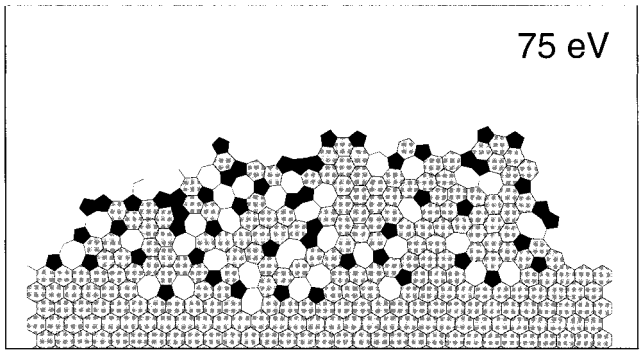

FIG. 4. Ring structure of the film grown with 75 eV ions. The color of each ring indicates the number of atoms in the ring: black (five atoms), gray (six atoms), and white (seven or more atoms).

Figure 5 demonstrates that the impacting ions do not ''subplant'' below the surface of the film, rather they form new surface material, with a coordination of two likely in over 50% of events. In addition, there is no correlation between the number of ions deposited into the bulk and the compressive stress. Also, the small number of events which did give rise to a subplanted atom were not due to direct subplantation, but to ''caving-in'' of nearby atoms when the ion was deposited into a small valley in the surface. These results are significant as they demonstrate that subplantation is not necessary to generate compressive stress. While it may be argued that subplantation may occur in three-dimensional structures, it cannot be presumed that the compressive stress is due to subplantation effects.

Figure 7 shows the average number of bonds formed and broken per impact in the surface and bulk regions as a function of the ion energy. The solid and dotted lines are linear and quadratic curve fits, respectively. A significant feature of this graph is that the number of bonds formed and broken in the bulk is the same, which shows that the energetic ions do not add net material to the bulk. Were this the case the implanted ions would produce a net increase in the number of bulk bonds, an effect which is not observed. This reinforces

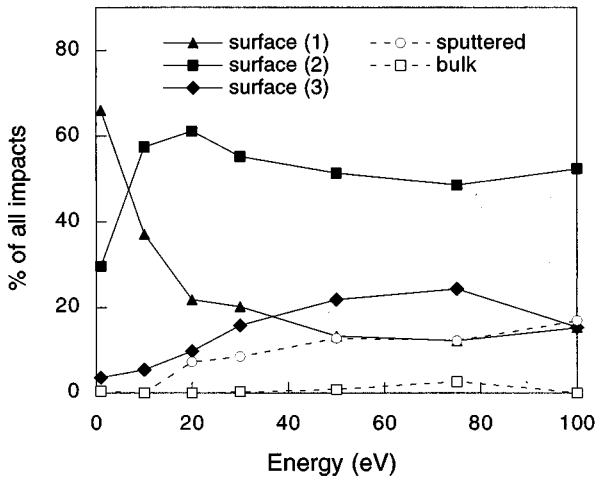

FIG. 5. Resting place of the energetic ions after impact as a function of energy. The bracketed numbers show the coordination of the ion on the surface. The distinction between surface and bulk was made using the convention shown in Fig. 6.

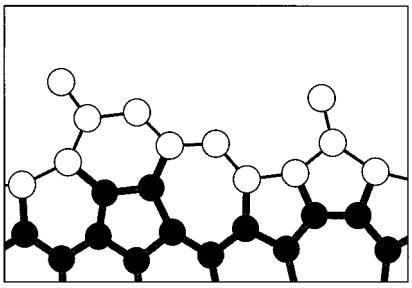

FIG. 6. Scheme used to identify atoms and bonds as belonging to either the surface or the bulk. The white circles represent surface atoms and the solid circles represent bulk atoms, while the thin and thick bonds denote surface and bulk bonds, respectively.

the argument presented above that subplantation does not occur and shows that the only process occurring in the bulk is annealing.

Further evidence for the surface growth model is reflected in the net number of surface bonds created. The difference in the number of surface bonds formed and created is approximately constant around 1.5 bonds/impact, which is the expected growth rate for a structure which is threefold coordinated. This demonstrates that the growth of the film occurs at the surface. The slight convergence of the two curves at higher energies is due to an increase in sputtering, which reduces the deposition rate.

The linear and quadratic dependence of the surface and bulk statistics are also worthy of mention. Such a dependence is consistent with the thermal spike radius r being proportional to the ion energy. This conclusion is based on the fact that in two dimensions the number of surface and bulk bonds lying within a distance r of the impact site scales as r and r^2, respectively.

It is interesting to speculate on the annealing mechanism responsible for the decrease in stress at higher energies. Referring to the curves showing the number of bonds altered in the bulk it is evident that the stress begins to decrease when the number of bonds annealed approaches 1 bond/impact. If

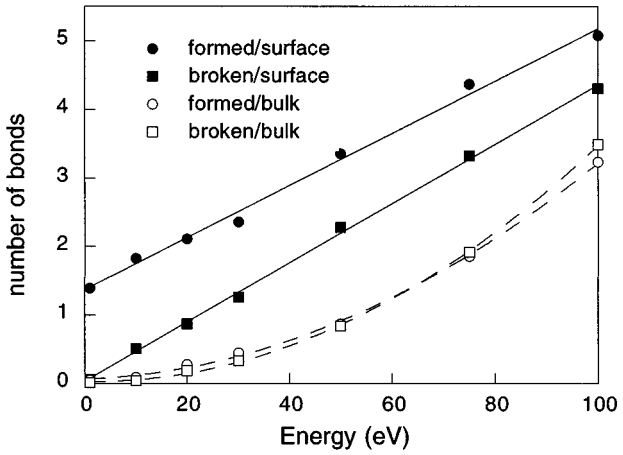

FIG. 7. Average number of bonds formed and broken per impact. The solid circles and squares denote bonds formed and broken on the surface. Similarly, the white circles and squares indicate bonds broken and formed in the bulk. The solid and dotted lines are linear and quadratic curve fits, respectively.

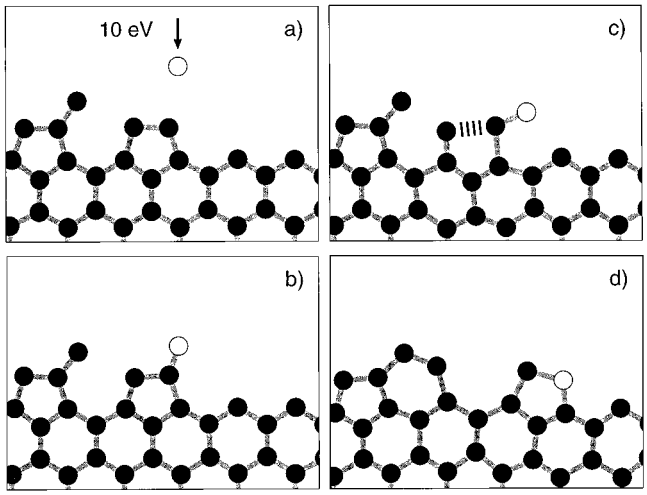

FIG. 8. Animation sequence showing various stages in the deposition of a 10 eV atom (white circle). The frames shown correspond to the following times: (a) 0 ps; (b) 0.01 ps; (c) 0.03 ps; (d) 0.08 ps.

the growth process is assumed to produce a mixture of compressed and tensile bonds, say 0.9 and 0.6 bonds/impact, then a critical value of 1 bond/impact appears to be a sensible point for the maximum compressive stress to be achieved. Above this energy the compressed bonds will be broken faster than they can be created and a lower stress will result. Evidence supporting a mixture of atoms under compressive and tensile stress in all films is reported in a later section using the local stress parameter σ_i.

C. Dynamics of the thermal spike

Animation sequences provide a useful insight into the deposition process and the interactions between the energetic ion and the surface of the film. A series of snapshots depicting impacts at 10, 30, and 75 eV are shown below. These three energies span the three significant regions in Fig. 2, that is, films with no stress, films with the maximum compressive stress, and films with a reduced compressive stress. The pictures and the accompanying discussion help explain the behavior of the thermal spike and the generation of compressive stress from an atomistic viewpoint.

1. 10 eV impact

Figure 8 shows an example of how bonds are broken and formed when an ion is deposited with an energy of 10 eV, which is approximately twice the strength of a bond. The ion, shown as a white circle, makes a glancing collision with a surface atom [Fig. 8(b)], which transfers momentum to a second surface atom immediately to its left [Fig. 8(c)], breaking the bond between them in the process. At this time the motion of the surface atoms has slowed somewhat but they still have sufficient energy to form two new ring structures [Fig. 8(d)], which are more stable than dangling bonds.

The surface nature of the impact is a clear feature of deposition at this energy. Both the bond which broke and the three new bonds formed lay on the surface, and the final position of the ion was also on the surface. Important information about the impact is seen in Fig. 9, which shows the kinetic energy of the incident ion during the deposition process. It is evident that the ion loses most of its kinetic energy in its first collision, and that the energy of the ion rapidly diffuses away into the substrate. The efficient transfer of energy occurs because all the atoms have the same mass.

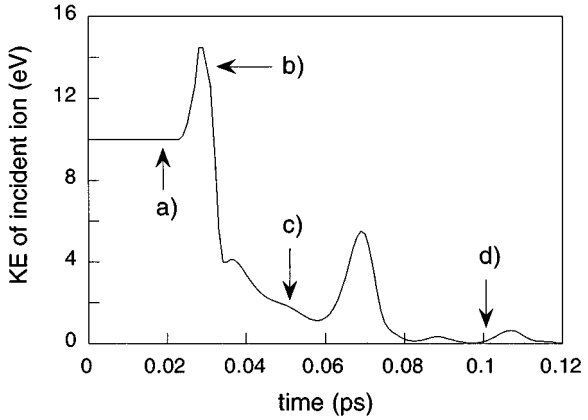

FIG. 9. Kinetic energy of the incident ion at the stages of the 10 eV ion impact depicted in Fig. 8.

The effects observed in this impact are even more pronounced at higher ion energies where they play a significant role in the growth of the film. The rapid transfer of energy produces temporary compression of the surface area due to the conversion of the ion's kinetic energy into potential energy in the film. When the compressed region expands, kinetic energy is released creating the thermal spike. The joint role played by the compressed region and the thermal spike are considered again in the Discussion.

Also worthy of note in Fig. 9 is the increase in the kinetic energy of the ion when it forms a bond. As the ion approaches the surface of the film, it is accelerated into the potential well of the closest atom, gaining nearly 5 eV of kinetic energy in the process. A similar increase occurs between Fig. 9(c) and Fig. 9(d) when the ion forms its second bond. At lower impact energies, such as at 1 eV, this extra kinetic energy provides additional surface mobility for the depositing ion.

2. 30 eV impact

Figure 10 shows an impact at 30 eV, the energy at which the compressive stress is a maximum. The new ion, drawn as a white circle, makes a head-on collision with a surface atom [Fig. 10(b)], which is displayed as a gray circle. The ion loses most of its energy to this grey atom, breaking the eight-membered ring which collapses downwards [Figs. 10(c) and 10(d)]. This leaves the ion with no surface to bond to and results in the sputtering of the ion. By this time sufficient energy has diffused into the substrate for the atoms to close into first a six-membered ring [Fig. 10(e)], and later, a five-membered ring [Fig. 10(f)].

The trajectory followed by the atom color-coded gray is of some significance. This atom is usually termed a ''knock-on'' atom as it receives the bulk of the energetic ion's kinetic energy. In the subplantation model such an atom would initiate a knock-on sequence and produce a subsurface interstitial, which in turn would increase the density and produce compressive stress. The simulation, however, shows this not to be the case. Instead, the knock-on atom initiates a rear-

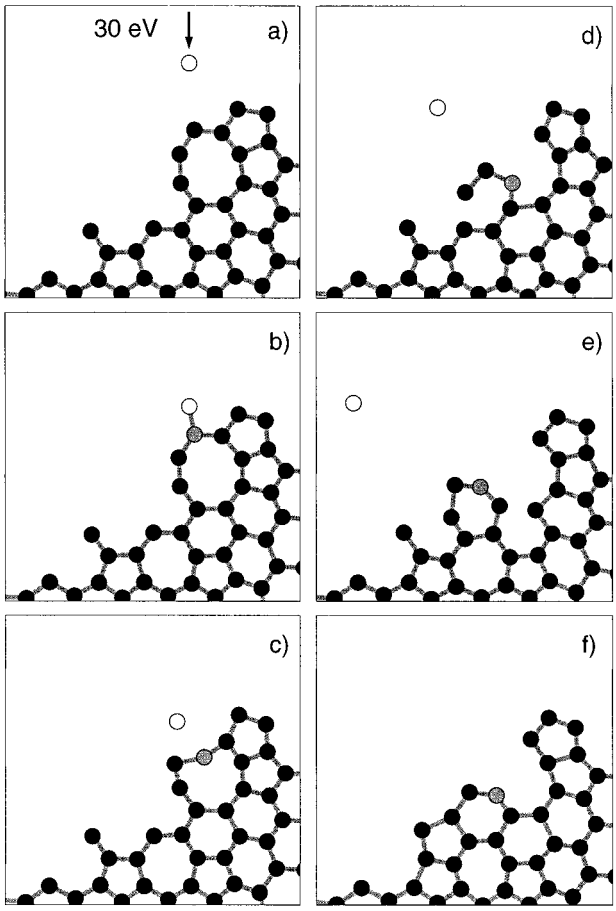

FIG. 10. Animation sequence showing various stages in the deposition of a 30 eV atom (white circle). The gray circle indicates the "knock-on" atom which receives the majority of the kinetic energy of the energetic ion. The frames shown correspond to the following times: (a) 0 ps; (b) 0.01 ps; (c) 0.02 ps; (d) 0.05 ps; (e) 0.10 ps; (f) 0.20 ps.

rangement of the surface, converting a weakly bonded eight-membered ring to the much stronger and denser combination of a five- and a six-membered ring.

Another important point is that as in the 10 eV case the impact is primarily a surface event, despite 30 eV being the energy at which the compressive stress is a maximum. A comparison of Figs. 10(a) and 10(f) shows that only two bonds were broken, both from the surface, and that of the three new bonds formed, two lay on the surface while the third was in the bulk. The presence of high compressive stress at 30 eV and the lack of surface penetration demonstrates that the compressive stress is formed at the surface when the energetic ions bury preexisting surface in a stressed configuration.

3. 75 eV impact

At higher energies the films grow with a reduced stress due to an annealing process. Figure 11 shows a section of film before and after the deposition of a 75 eV atom. This single impact considerably alters the surface, breaking three rings and forming five new ones. The plus and minus signs indicate the rings which were formed or broken as a result of the impact.

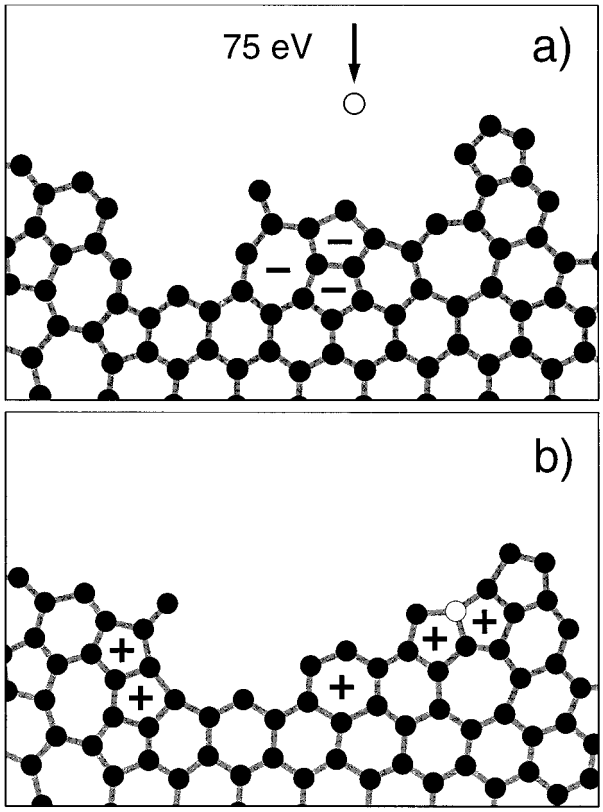

FIG. 11. Section of film before (a) and after (b) the deposition of a 75 eV ion, shown as a white circle. The plus and minus signs indicate rings formed or broken as a result of the impact.

It is evident that the 75 eV impact is considerably more energetic than the impacts at lower energies. Six bonds were broken, and nine new bonds were formed, some of which lay 9 Å away from the impact site. Of greater importance, however, is that of the six bonds broken, two were bulk bonds, which is of relevance to the stress relieving mechanism. At lower energies very few bonds are broken in the bulk, but as shown in Fig. 7, the number of bonds broken in the bulk increases significantly with increasing energy. The simultaneous increase in broken bulk bonds and decrease in stress suggests that the breaking of bulk bonds is the factor responsible for reducing the stress at higher energies. One feature which the 75 eV impact does share with the lower energy impacts is that the energetic ion comes to rest on the surface of the film.

D. Microscopic view of stress

The local stress parameter σ_i provides a useful and intuitive interpretation of the stress in the films. In particular, pictures of the films using σ_i highlight the compressive and tensile stressed areas and the interaction between the film and substrate. Figure 12 shows three films, with the circles and dots indicating the local stress at each atom. The solid circles denote a compressive stress, the white circles a tensile stress, and the small dots a neutral stress.

The stress in the films is reflected in the stress pattern in the substrate. For the tensile stressed 1 eV film, the tendency of the film to contract squeezes the section of substrate beneath it. This squeezing action produces the semicircular

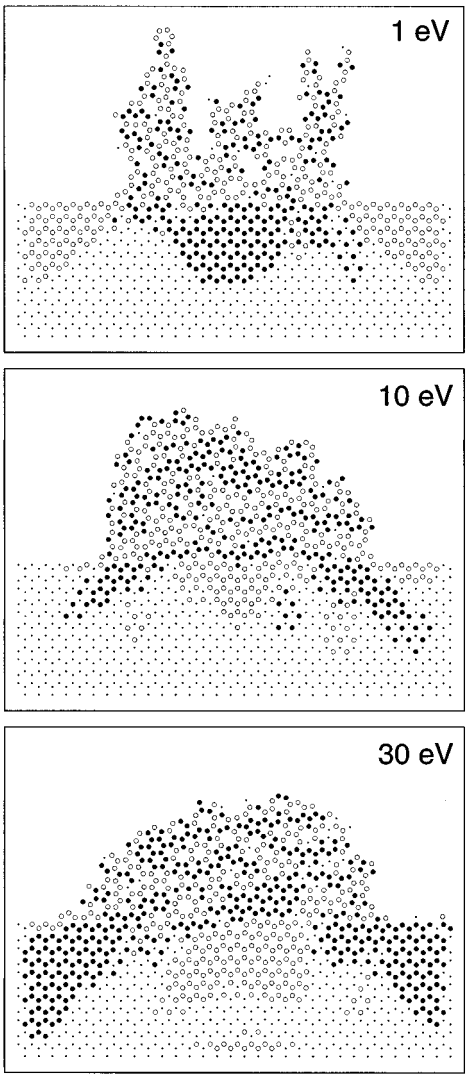

FIG. 12. Films grown with 1, 10, and 30 eV ions displayed using the local stress parameter σ_i. The solid circles, small dots, and white circles indicate compressive, neutral, and tensile stresses, respectively.

compressively stressed region (solid circles) below the film. The opposite effect is seen between the edge of the film and the fixed substrate boundaries. On either side of the film are triangular-shaped regions of the substrate which are tensile stressed (white circles). This tensile stress, which indicates these parts of the substrate are being stretched, is due to the contraction of the central section of the substrate.

For the compressively stressed 30 eV film the situation is reversed. In this case the film is trying to expand, which produces a tensile stress (white circles) in the central section of the substrate. Accordingly, the expanded central section results in a compression of the substrate near the boundary. The triangular region of compressively stressed atoms (solid circles) on either side of the film reflect this squeezing. The film grown with 10 eV ions is essentially unstressed and hence does not produce a significant stress pattern in the substrate.

An important feature of Fig. 12 is that all three films contain a large number of both compressive and tensile stressed atoms despite having significantly different total

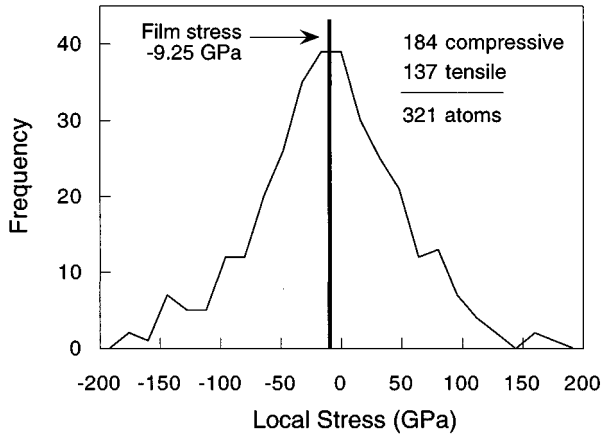

FIG. 13. Distribution of local stress in the film grown with 50 eV ions. The average stress is indicated by the solid vertical line.

stresses. The distribution of local stresses in the film grown with 50 eV ions is seen in Fig. 13. The thick vertical line shows the total film stress, which by Eq. (2) is the average value of the local stresses. Despite the broad distribution of local stresses, there is a clear excess of compressively stressed atoms resulting in a total stress which is compressive. A similar distribution of local atomic stresses has been obtained by Kelires,[14] who used a Monte-Carlo annealing technique to simulate the elastic properties of *ta*-C.

This broad distribution of stresses reflects the large range of bond lengths present in the films as well as induced stress effects. In regions where the film is compressively stressed a tensile stress is induced in the film below, and *vice versa*, an effect similar to the film-substrate interaction discussed above.

This presence of significant numbers of compressive and tensile areas demonstrates that the stress generation mechanism is more subtle than most models suggest. The films are not compressively stressed because the impacts always produce densification, rather the stress arises because the growth process produces a film with more compressively stressed atoms than tensile stressed atoms.

An important part of the technique used to measure the total stress was a curve fitting procedure used to account for fluctuations in the film stress with thickness. As shown in Fig. 14, the stress in the film (the thin solid line) does not reach a constant value until several hundred atoms have been deposited. In addition, the fluctuations increased with energy making the curve fitting procedure (shown as a thick dotted line) a valuable tool at higher energies. A second feature of the thickness dependence of the stress was the linear change in stress from an initial tensile value to the constant average compressive value. This trend was present in all the films except the film grown with 1 eV ions. In fact, it was not possible to use the curve fitting procedure for the 1 eV film as the lack of periodic boundary conditions meant the stress peaked, then slowly decreased with thickness. The stress value plotted in Fig. 2 is the stress after all 300 atoms were deposited.

IV. DISCUSSION

The results presented above allow us to make a number of assertions about the mechanism which produces compressive

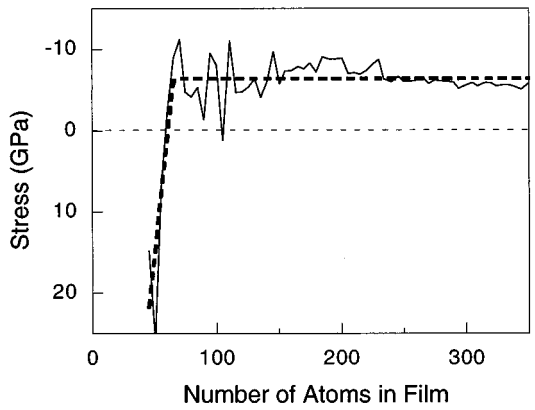

FIG. 14. Stress in the film grown with 20 eV ions as a function of the number of atoms in the film. The thick dotted line shows the curve fit used to extract average film stresses.

stress in a two-dimensional system. While the generalization to three dimensions requires some care, the agreement between experiment and the simulations suggests the essential physics will be similar.

A major observation in this work is that the stress generation process is more subtle than previously thought. For this reason it is almost as important to state what does not produce stress as what does. The traditional picture of the energetic ion inserting itself into the subsurface of the growing film is not supported by the simulations (Figs. 5 and 7), neither is there any evidence for the related mechanism of knock-on subplantation (Fig. 10). Another key point concerns the statistical nature of the stress generation mechanism. Analysis of individual atomic sites reveals a broad range of compressive and tensile stresses (Fig. 13), which sum to give a much smaller net stress.

It is significant that compressively stressed films are produced even though the energetic ions do not penetrate the surface. Instead the stress is a consequence of the growth process itself. When the energetic ion strikes the surface it distorts and compresses a small region and loses most of its kinetic energy in the process (Fig. 9). The compressed region expands a fraction of a picosecond later, converting the potential energy associated with the compression into kinetic energy. This kinetic energy rapidly diffuses away and the disordered region becomes sufficiently cool and forms a structure which conforms to the topology of the system. If sufficient kinetic energy was available, the region would be able to self-anneal and a neutral stress condition would result. However, by the time the region is cool enough to form a solid structure, most of the kinetic energy which was associated with the distortion has diffused away. Thus the process is irreversible as the surface region has less kinetic energy to relieve the distortion than was used to create it. This leads to a ''locking-in'' of the compressively stressed structure and subsequent ions cannot ''unlock'' this structure unless they have a much larger energy.

Another important point is that this locking-in of the stressed structure is an inherently collective phenomenon involving the cooperative behavior of a number of atoms. It cannot be viewed as a process resulting from the motion of one atom only. Models which picture the new ion inserting into a preexisting structure ignore the strong interactions which result in the complete disruption of the structure.

V. CONCLUSION

In summary, the simulations performed in this work demonstrate that in two dimensions the compressive stress in thin films is not due to the implantation of energetic ions. We propose a model of film growth in which the energetic ions grow new surface which is compressively stressed due to an equilibrium between impact-induced compression and thermal spike annealing. It is also shown that at the atomic level the stress in the films is considerably inhomogeneous, and that the films contain significant numbers of tensile and compressively stressed atoms. This mixture of tensile and compressive stress is not predicted by film growth models which explain the stress simply in terms of densification.

ACKNOWLEDGMENTS

The authors wish to thank ANSTO for provision of considerable CPU time on their Fujitsu VP-2200. Thanks also go to VisLab at The University of Sydney for access to extensive visualization resources. The authors acknowledge financial support from the Science Foundation for Physics within Sydney University.

[1] D. R. McKenzie, D. Muller, and B. A. Pailthorpe, Phys. Rev. Lett. **67**, 773 (1991).
[2] D. R. McKenzie, W. D. McFall, W. G. Sainty, C. A. Davis, and R. E. Collins, Diamond Related Mater. **2**, 970 (1993).
[3] C. A. Davis, Thin Solid Films **226**, 30 (1993).
[4] J. Robertson, Pure Appl. Chem. **66**, 1789 (1994).
[5] K.-H. Müller, J. Appl. Phys. **62**, 1796 (1987).
[6] H.-P. Kaukonen and R. M. Nieminen, Phys. Rev. Lett. **68**, 620 (1992).
[7] J. Tersoff, Phys. Rev. Lett. **61**, 2879 (1988).
[8] B. A. Pailthorpe, J. Appl. Phys. **70**, 543 (1991).
[9] B. W. Dodson, Phys. Rev. B **36**, 1068 (1987).
[10] F. Stillinger and T. A. Weber, Phys. Rev. B **31**, 5262 (1985).
[11] A. Bensan, Honours thesis, University of Sydney, 1990.
[12] C. C. Fang, F. Jones, R. R. Kola, G. K. Celler, and V. Prasad, J. Vac. Sci. Technol. B **11**, 2947 (1993).
[13] I. I. Aksenov, A. N. Belokhvostikov, V. G. Padalka, N. S. Repalov, and V. M. Khoroshikh, Plasma Phys. Controlled Fusion **28**, 761 (1986).
[14] P. C. Kelires, Phys. Rev. Lett. **73**, 2460 (1994).